Calibration of near-infrared frequency-domain tissue spectroscopy for absolute absorption coefficient quantitation in neonatal head-simulating phantoms

Brian W. Pogue
Keith D. Paulsen
Thayer School of Engineering
Dartmouth College
Hanover, New Hampshire 03755

Chris Abele
Howard Kaufman
Innervision Diagnostics
Newton, Massachusetts 02459

Abstract. Frequency-domain tissue spectroscopy is a method to measure the absolute absorption coefficient of bulk tissues, assuming that a representative model can be found to recover the optical properties from measurements. While reliable methods exist to calculate absorption coefficients from source-detector measurements less than a few centimeters apart along a flat tissue volume, it is less obvious what methods can be used for transmittance through the larger tissue volumes typically associated with neonatal cerebral monitoring. In this study we compare the use of multiple distance frequency-domain measurements processed with (i) a modified Beer–Lambert law method, (ii) an analytic infinite-medium diffusion theory expression, and (iii) a numerical finite element solution of the diffusion equation, with the goal of recovering the absolute absorption coefficient of the medium. Based upon our observations, the modified Beer–Lambert method provides accurate absolute changes in the absorption coefficient, while analytic infinite-medium diffusion theory solutions or finite element-based numerical solutions can be used to calculate the absolute absorption coefficient, assuming that the data can be measured at multiple source-detector distances. We recommend that the infinite-medium multi-distance method or the finite element method be used across large tissue regions for calculation of the absolute absorption coefficient using frequency-domain near-infrared measurements at multiple positions along the head. © *2000 Society of Photo-Optical Instrumentation Engineers.* [S1083-3668(00)00402-0]

Keywords: photon migration; diffusion theory; diffuse; hemoglobin; saturation.

Paper JBO-90003 received Jan. 14, 1999; accepted for publication Nov. 22, 1999.

1 Introduction

Near-infrared spectroscopy (NIRS) is a tool for monitoring hemoglobin dynamics in vivo, which is used clinically for finger and toe pulse oximetry, jugular venous pulse oximetry,[1,2] as well as for applications in muscle,[3,4] neonatal cerebral oximetry,[5,6] fetal oximetry before or during labor[7–10] and adult patient monitoring during cardiopulmonary bypass surgery.[11,12] In the last ten years, research and development in this area has grown in parallel with new applications, which has led to a range of instruments possessing different levels of utility.[13] The geometry of the source-detector position and the measurement process itself play important roles in determining what precise characteristics of the hemoglobin/blood are measured. While pulse oximetry simply determines the oxygen saturation in the arterial blood through the finger or toe, devices placed on the head or arm measure spatially averaged changes in oxygen saturation and blood volume in the tissue. Recently, there has been an effort directed towards developing clinical devices to measure the absolute hemoglobin concentration and oxygen saturation, rather than only changes or trends in these parameters. The calibration of these latter in-

struments is distinctly different than that of trend monitors, and is still the subject of ongoing research. This paper investigates how to calibrate such a monitor, which uses frequency-domain light measurement through thick tissues to calculate absolute absorption coefficients of the tissue and thereby absolute hemoglobin concentration values.

Perhaps the most successful optical hemoglobin monitor is the pulse oximeter which is easy to calibrate and is well established in the clinic, but comes at the expense of yielding limited information. Pulse oximeters can provide quantitatively accurate readings of arterial hemoglobin saturation within the range of 70%–100%, but fail when used outside this range, and cannot determine blood volume changes nor venous blood dynamics.[1,2,10,14,15] More advanced systems which measure the near-infrared transmission through thick regions of tissue can be used to quantify changes in blood volume and blood oxygen saturation.[16] However, these systems are also limited to applications where the absolute value of blood volume and blood oxygenation is not needed, or where pre-calibration in vivo will suffice.[17] While there are many published reports showing successful application of this technology, there are also a large number of studies which have demonstrated the inability of commercial NIRS oxygen

Address correspondence to Brian W. Pogue, Thayer School of Engineering, Dartmouth College, Hanover, NH 03755. Electronic mail: pogue@dartmouth.edu

monitors to produce accurate results in patients.[11,12,18–20] This problem is likely due to the limited range of oxygen dynamics over which the instrument is calibrated, and the inability of continuous wave systems to accurately account for pathlength changes in the tissue. The most desirable solution to this problem is the development of newer systems which measure the tissue optical pathlength directly and do not need empirical calibration.

Systems which directly measure the optical pathlength through tissue can be used to determine quantitatively accurate hemoglobin concentrations by direct calculation of the tissue absorption coefficient at several different wavelengths. This approach has clinical benefits in cerebral blood saturation monitoring where the hemoglobin dynamics are more complex[21] and where inter-patient variability is a large problem.[22,23] Unfortunately, these more complex NIRS systems, which can measure the optical pathlength through tissue and quantify hemoglobin concentrations, require more calibration, modeling and a careful evaluation of their applicability, in order to be useful.[13,24–27] Thus, while the applications of pathlength measuring NIRS oximetry systems are many and promising, each system requires detailed calibration and testing to validate its utility in specific situations.

Systems for measuring the optical pathlength in vivo can be separated into spectrally resolved,[26,28] spatially resolved, time-resolved[29–31] and frequency-domain devices,[4,32–34] which differ mainly in the technology used to create and detect the light. The latter approach uses light intensity signals which are rapidly oscillated to measure the path of travel through the tissue by the phase shift in the detected signal. This approach provides a workable system for neonatal monitoring since it can be designed relatively inexpensively, can be used for measurements across large tissue volumes, and under certain conditions can be used to calculate the absorption coefficient of the tissue in a manner which is insensitive to irregular boundary conditions.[35]

One important calibration issue is to determine the conditions under which accurate absorption coefficients can be determined from frequency-domain measurements in tissue geometries such as the neonate head. In general, some model of light propagation must be adopted to match the experimental data to theoretical predictions in order to estimate tissue optical properties. Perhaps the simplest model which may be applied is the modified Beer–Lambert Law[36,37] which can be used with a direct probe of the optical pathlength that the light has traveled in tissue. Another possible solution is to use analytic diffusion theory to predict the light signal,[31–33,35,38] along with relative rather than absolute measurements in order to minimize differences due to boundary effects. This approach can work well for relatively small source-detector distances (approx. 1–5 cm),[39,40] but it is not clear how well it will work for highly curved tissues which are not modeled well analytically.[35] For these larger tissue volumes, more complicated numerical methods must be used to solve the diffusion equation with boundaries which closely approximate the real tissue geometry.[41–43] These three model-based methods—(i) Beer–Lambert law, (ii) analytic infinite-medium diffusion theory, and (iii) numerical diffusion theory calculation with curved boundaries—are examined here on a series of data sets taken from tissue simulating phantoms with well characterized optical properties, to determine which approach will pro-

Fig. 1 Photograph of the apparatus for neonatal cerebral hemoglobin monitoring. The black cables are fiberoptic bundles for delivery and detection of the light. The instrument uses frequency-domain light to measure intensity and phase shift of the near-infrared light through a distance of tissue.

vide an accurate and robust method of estimating the absorption coefficient.

2 Materials and Methods

2.1 Instrumentation

Two instruments were used in this work, which had the same type of frequency domain light source and detection methods. The first system was a compact unit developed by Innervision Diagnostics designed for clinical monitoring of neonatal cerebral hemoglobin concentration and oxygen saturation using a single source and detector fiber (see Figure 1 for photograph). The second system was an imaging array using 16 source and 16 detector positions in a circular annulus, which was developed for breast cancer imaging of hemoglobin and can be seen in previous references.[44,45] Both sets of instrumentation used frequency-domain light signals at 750, 800, and 833 nm, which were multiplexed into optical fiber bundles. The lasers were powered by both dc current drivers as well as ac current driven in the 100–300 MHz range. Light detection was achieved through photomultiplier tubes (R928, Hamamatsu Inc.), with rf modulated housings to heterodyne the signal

down to the range of 100–1000 Hz frequency (ISS Instruments, Champaign-Urbana, IL), so that it could be sampled by an analog/digital (A/D) board in the computer. The single source and detector fiber bundles on the compact clinical system were 3 mm in i.d. and approximately 12 ft long for ease of attachment to patients. The multiple source-detector system used 2 mm plastic fibers for the source light, and 6 mm silica fiber bundles for the detected light and were all fixed in a circular array where the diameter could be varied.[45] In this multiple fiber array, multiplexing of the source-detector locations was achieved through mechanical translation of the light source and detector into the different bundles, via linear translation stages controlled by the computer.[44] Preliminary data obtained with the two systems demonstrated that both the phase shift, ϕ, and ac amplitude, I_{ac}, were similar (to within 5%) when measured across the same tissue simulating phantoms for the same geometry of source fibers. Since the detection hardware was identical for the two systems, measurements from the two were used interchangeably.

2.2 Tissue Phantoms

Calibration measurements were carried out on tissue simulating phantoms consisting of Intralipid, diluted to 0.5% by volume in water, which is considered to represent the scattering coefficient of tissues reasonably well.[46] The absorption coefficient of this solution in the near infrared is essentially all due to water, so that varying amounts of human blood can be added to the phantom to simulate the optical properties of tissue. Samples of blood were obtained from adult human volunteers, and evaluated for oxygen and hemoglobin content in a clinical co-oximeter and blood gas machine (Chiron Diagnostics Inc., Model 855). Hemoglobin content in all blood samples was 15.6 ± 0.1 g/dL, and this value was used to calculate the molar absorption coefficient of our blood samples at the three pertinent wavelengths, using published values of reduced hemoglobin, Hb-R, and oxygenated hemoglobin, Hb-O$_2$, molar absorption coefficients from Wray et al.[47] The phantom solution was contained in different nalgene plastic containers with diameters between 60 and 95 mm. The container walls were scattering enough to allow light transmission through the container, while minimizing the lateral transmission of light through the walls directly to the detectors, so that all detected light can be assumed to have passed through the scattering medium 40. Preliminary studies indicated that the container walls produced a constant offset in the absorption coefficient which could be pre-calibrated[45] (data not shown).

3 Theoretical Methods

3.1 Modified Beer–Lambert Law Using the Differential Pathlength Factor

Much of the initial development of current neonatal monitors has been reported by Cope and Delpy.[36,48] The concept of measuring the pathlength of light propagation through tissue has been discussed in detail by this group, and several studies have shown that the optical pathlength in neonatal brain is 4–7 times the optical pathlength through nonscattering media.[23,24,49] Cope et al. have shown that absolute changes in the absorption coefficient, μ_a, can be determined through arbitrary shaped tissue volumes using a modified Beer–

Lambert law.[37] In this method, the logarithm of the transmitted intensity, I, is used along with a measure of the optical pathlength, l_P, in the equation

$$\ln(I/I_o)=-l_p\mu_a+G, \tag{1}$$

where I_o is the initial intensity before entering the tissue and G is a constant factor related to the geometry of the tissue. When data from multiple detector positions are available, it is possible to consider the spatial derivative of Eq. (1) to minimize G and potentially calculate μ_a, from the equation

$$\frac{d\ln(I)}{d\rho}=-\frac{dl_P}{d\rho}\mu_a+\frac{dG}{d\rho}, \tag{2}$$

where ρ is the distance along the tissue between source and detector. Here, the spatial derivative of the optical pathlength is equivalent to the differential pathlength factor (DPF) described by Cope and Delpy.[37] If the geometrical factor G is not highly spatially dependent, then the latter term in Eq. (2) may produce an insignificant offset. In the following work, the spatial derivative of the pathlength factor was calculated by measurement of the phase shift, ϕ, as a function of distance, ρ, compared to the phase shift in nonscattering media

$$DPF=\frac{dl_P}{d\rho}=\frac{d\phi}{d\rho}\frac{c}{\omega}, \tag{3}$$

where c is the speed of light in the medium, and ω is the modulation frequency times 2π. Equations (2) and (3) were used to calculate μ_a under the assumption that $dG/d\rho$ was negligible, but the validity of this assumption will be discussed further below.

3.2 Analytic Infinite-Medium Diffusion Theory

The propagation of light in tissue is well described by radiation transport theory, and its simplification to the highly scattering regime results in the diffusion equation. This equation can be solved analytically for simple geometries such as the infinite medium, semi-infinite, slab, sphere and cylinder,[35,38,50] providing solutions which are more exact than the modified Beer–Lambert law. These analytic solutions can be used with light measurements of phase and amplitude to calculate absorption and scattering coefficients, assuming that the tissue geometry is regularly shaped. Fantini et al.[33] have demonstrated that a diffusion theory model can be used reliably to fit changes in phase shift and logarithm of the intensity for source-detector distances ranging from 3 to 5 cm. It is not obvious how well this model will work for larger source-detector distances, or for tissue geometries with a high degree of curvature. One benefit of the analytic solution method proposed by Fantini et al. is that multiple source or detector locations can be used, to approximate the spatial derivatives of the phase shift and intensity ratio which can be fit to their analytic counterpart in order to estimate μ_a and μ_s'. In particular, for this work we used the expressions

$$\frac{d\phi}{d\rho}=(\mu_a/D)^{1/2}[1+(\omega/\mu_ac)^2]^{1/4}$$
$$\times\sin[\tan^{-1}(\omega/\mu_ac)/2], \tag{4}$$

$$\frac{d(\ln(\rho I_{ac}))}{d\rho}=(\mu_a/D)^{1/2}[1+(\omega/\mu_a c)^2]^{1/4}$$

$$\times\cos[\tan^{-1}(\omega/\mu_a c)/2] \qquad (5)$$

where I_{ac} is the ac intensity measured by the detector, D is the diffusion constant defined as $D=(3\mu_s')^{-1}$, and ρ is the chord distance between source and detector.[51] These expressions [Eqs. (4) and (5)] are matched to measurements of phase shift versus distance and $\ln(\rho I_{ac})$ versus distance to derive μ_a and μ_s' values.

Diffusion theory solutions for the infinite medium, semi-infinite plane, and infinite slab are also compared to experimental measurements in an effort to investigate the accuracy of these solutions in curved tissue-simulating phantoms. In this case, the analytic solution for a cylinder or sphere could be used; however, these expressions require the summation of an infinite series of Bessel functions, which requires significantly more computation, and does not lend itself well to iterative determination of μ_a and μ_s'. A more flexible alternative to these analytic solutions is to solve the equation numerically on an arbitrary boundary with the finite element method.

3.3 Numerical Diffusion Theory

Numerical solution of the diffusion equation has been used successfully with circular tissue regions, and has formed the basis for tissue imaging when coupled to an appropriate inverse solver. In the imaging context, either a finite difference[42] or a finite element[43] solution of the frequency-domain equation can be used to calculate the predicted light fluence rate in a tissue region once the boundaries of the region are known and incorporated into the calculations. This approach has not been exploited in clinical monitoring, largely because of the complexity of the model, and the desire to find simpler solutions. In this study, finite element calculations are evaluated to determine the benefits of using a numerical forward solution of diffusion theory for monitoring, and to provide a basis for comparison with the two simpler analytic methods described above. Briefly, a Galerkin formulation of the frequency-domain diffusion equation was solved on a circular domain mesh, which could be scaled to the diameter of the phantom being imaged.[43] Measurements of phase shift and ac amplitude were calculated at node positions corresponding to the detector locations on the tissue-simulating phantoms. The homogenous optical properties of the simulation were fit to the experimentally measured values, using a Newton–Raphson method. Essentially this fitting procedure minimized the difference between experimental and theoretical values of the difference in phase shift and I_{ac} between neighboring detector sites.[45]

4 Results

4.1 Source-Detector Distance

A solution of 0.5% Intralipid with 12 ml/L of blood was prepared and contained in a 72-mm-diam cylindrical phantom. Measurements of phase shift and ac intensity were made at different source-detector separations around the perimeter, using a modulation frequency of 100 MHz and a wavelength of 750 nm. These measurements are plotted as points in Figure
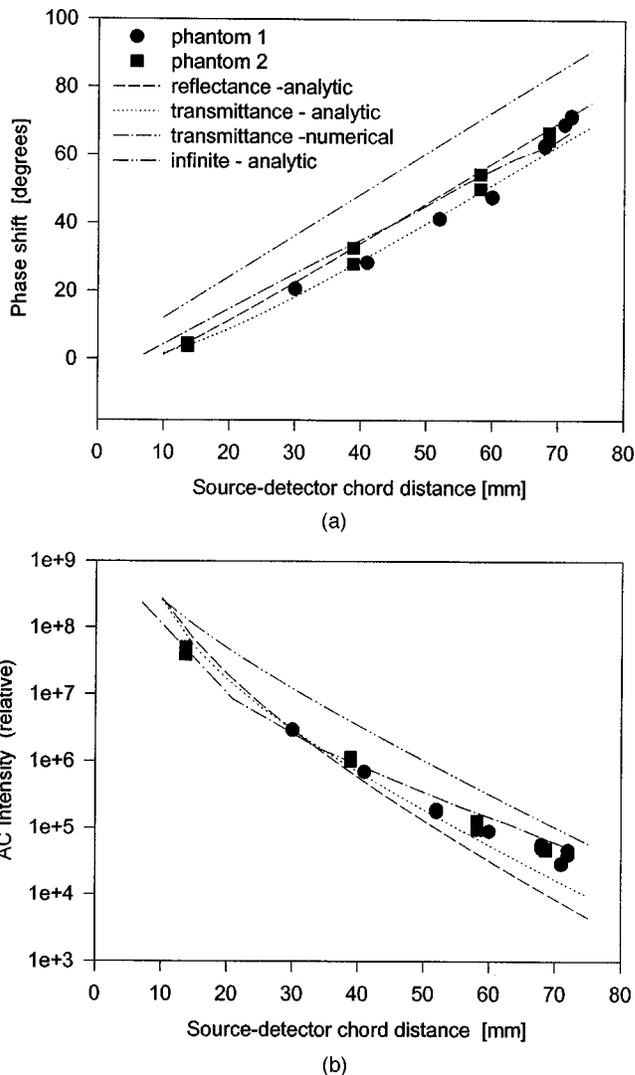
Fig. 2 Plots of phase shift (a) and ac intensity (b) vs the chord distance between source and the detector locations. Experimental data from two phantoms with the same optical properties are shown. The lines are predictions from analytic diffusion theory for (i) reflectance and (ii) transmittance from a slab, (iii) numerical finite element calculations for a cylinder and (iv) analytic infinite medium calculations. Note that the phase was referenced to zero when source detectors were placed together, and the ac intensity data are relative only, and fit to match the calculated transmittance-numerical line.

2, along with lines representing calculations of phase shift and ac intensity, from four different theoretical models: (i) analytic reflectance from a thick slab, (ii) analytic transmission through a thick slab, (iii) transmission in the cylindrical geometry using a finite element solution, and (iv) analytic transmission through an infinite medium. Chord distances from source to detector of 14–72 mm were possible with this phantom cylinder. The measurements were repeated on two separate phantoms with different wall optical properties. Both sets of experimental data are plotted on the figure, and show little variation between them. A general observation from these calculations is that the slopes of all four of the diffusion theory models are quite similar, suggesting that any of them could be used to match the slope of the experimental data.

(a)

(b)
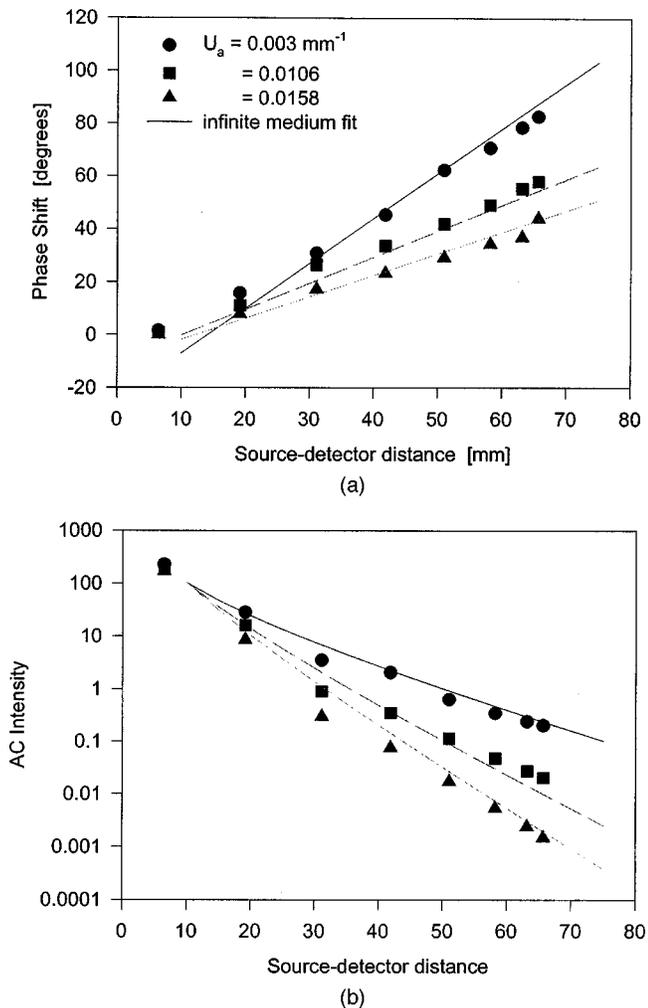
Fig. 3 Measurements of (a) phase shift and (b) ac intensity for three phantoms with different absorption coefficients, and a fixed scattering coefficient of $\mu_s'=0.51$ mm^{-1}. The lines are theoretical predictions from an infinite medium diffusion theory expression which have been scaled vertically to match the data (but the slope was fixed in each case).

In a similar cylindrical phantom with a 66 mm diameter, the same distance measurements were recorded on three different phantom compositions, covering a range of absorption coefficients which are typical of neonatal tissue in the near infrared.[36,48,52] In Figures 3(a) and 3(b) the ac intensity and phase shift are plotted, respectively, as a function of distance for the three phantom solutions where the scattering coefficient (i.e., Intralipid concentration) has been maintained at $\mu_s'=0.05$ mm^{-1}, and the three concentrations of blood (0.0, 17.0, and 29.0 ml blood per liter of solution) producing absorption coefficients of $\mu_a=0.0030$, 0.0106, and 0.0158 mm^{-1}. The points on the graphs are measured data, while the lines are based on calculations of the analytic infinite-medium expression for the fluence rate, using the expected μ_a and μ_s' values. The lines were scaled to fit the data by subtracting an offset in the phase and normalizing the intensity value by a constant, such that the slopes of phase shift versus distance and $\ln(I_{ac})$ versus distance were not altered. In general, there is a reasonably good fit between the calculated slopes and the
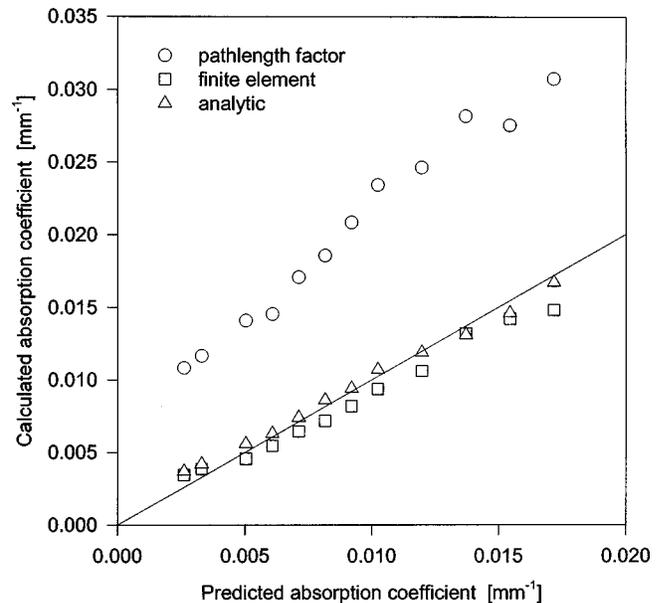
Fig. 4 Calculated absorption coefficient from a series of tissue-simulating phantoms using the three theoretical methods of (i) the modified Beer–Lambert law, (ii) analytic infinite-medium diffusion theory, and (iii) a finite element-based diffusion theory.

experimental data. Interestingly, the fits appear to be better at larger source-detector distances than at smaller source detector distances, indicating that transmission through the phantom across the full diameter is a better match to the infinite-medium calculation.

4.2 Comparison of Methods to Calculate the Absorption Coefficient

As described earlier, we have considered three methods of recovering the absorption coefficient of the medium based upon frequency domain measurements: (i) the modified Beer–Lambert law method, (ii) analytical infinite-medium diffusion theory and (iii) numerical diffusion theory based upon a finite element method (FEM). Both the analytical diffusion theory and the numerical diffusion theory solutions were iteratively solved using a Newton–Raphson algorithm to fit homogeneous values of μ_a and μ_s' to the spatial derivatives of phase shift and $\ln(\rho I_{ac})$. All three methods were tested for their ability to recover the absolute absorption coefficient of a series of phantom solutions with increasing blood concentration. The expected absorption coefficient values were calculated based upon the known optical properties of hemoglobin and water. The resulting absorption coefficient values are plotted in Figure 4, with the theoretical best fit presented as a solid line. The pathlength factor method exhibited a constant offset from the expected value, which was significantly high enough that it cannot be ignored. The other two diffusion theory based methods provided accurate estimates for all phantoms to within 10% of the expected values for the range of blood concentrations examined here.

(a)

(b)
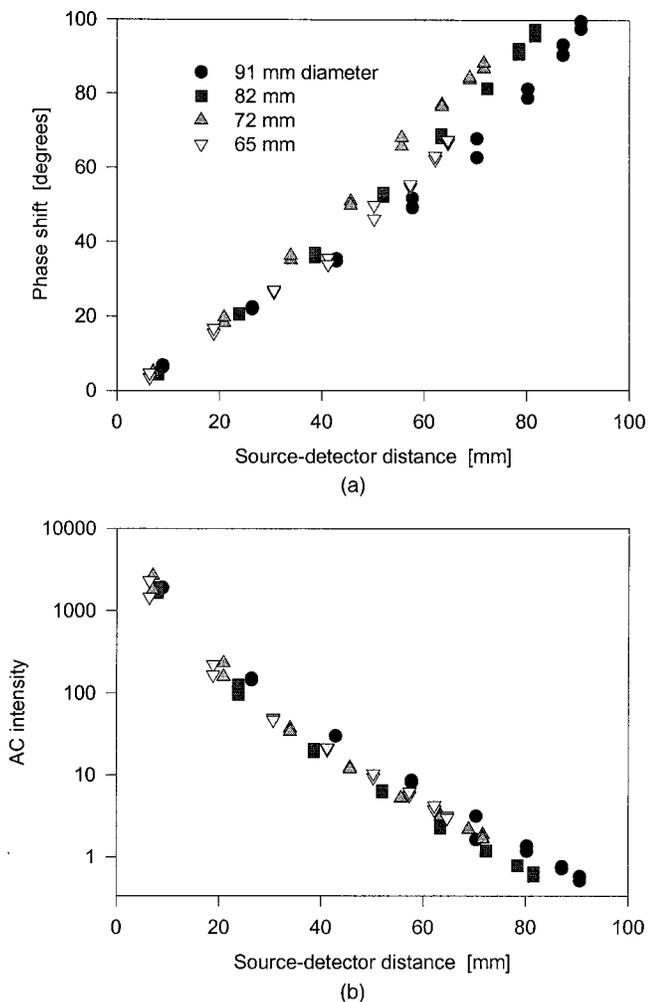
Fig. 5 (a) Phase shift vs distance measured from four cylindrical tissue-simulating phantoms with different diameters having the same material, $\mu_a = 0.0035$ mm^{-1} and $\mu_s' = 0.5$ mm^{-1}. (b) Measured ac intensity from the same phantoms. The distance plotted here is the chord between source and detector locations.

4.3 Effect of Different Sized Tissue Phantoms

The ability of the multi-distance infinite-medium method to accurately estimate phantom optical properties is encouraging; however, it is important to determine if the dimensions of the tissue phantom are a significant factor in fitting the data. To examine this issue, four different sized cylinders were used to hold the same tissue-simulating liquid phantoms, with fixed optical properties. Measurements of phase shift and ac intensity magnitude were taken from the phantoms, and the results are plotted in Figure 5, as a function of the chord distance between source and detector locations. In this case, the data from different sized phantoms show a slight spread in absolute values; however, the slopes of phase shift versus distance are constant to within 15%, as are the slopes of the logarithm of distance times the ac amplitude [i.e., $\ln(\rho I_{ac})$]. These spatial derivatives (slopes) were used to calculate the phantoms' optical properties with the three theoretical methods. The resulting optical properties are listed in Table 1. Again the pathlength method manifests a significant offset from the expected values while the analytic infinite medium

Table 1 Calculated values for absorption and scattering coefficients (in units of mm^{-1}) from three theoretical methods for processing the frequency-domain data. Note that the differential pathlength factor method does not recover a scattering coefficient. The expected values for the phantom were $\mu_a = 0.0037$ mm^{-1}, and $\mu_s' = 0.50$ mm^{-1}.

Diameter	μ_a (DPF)	DPF	μ_a (fem)	μ_s' (fem)	μ_a (infinite medium)	μ_s' (infinite medium)
91 mm	0.013	7.0	0.0040	0.47	0.0046	0.33
82 mm	0.012	7.9	0.0038	0.54	0.0042	0.39
72 mm	0.012	8.2	0.0040	0.57	0.0039	0.40
65 mm	0.014	6.7	0.0040	0.46	0.0043	0.29

approach agrees well with the finite element fitting scheme. Another observation from this data set is that the slope varies slightly depending upon the angle between the source and detectors suggesting that the optical property estimates would depend on the source-detector arrangement. This hypothesis was tested by processing the data from the 91-mm-diam phantom with the infinite medium derivative method where the fits for μ_a and μ_s' were based on different ranges of angles between source and detectors. The results are reported in Table 2 and show that the fitting is more accurate for source-detector angles which are greater than 90° (i.e., such that the source and detectors are on opposite sides of the phantom). This consideration may be quite important in the design of source-detector arrays using the infinite medium algorithm.

4.4 Effect of an Optically Clear Layer in the Medium

Recently there has been a significant amount of computational and experimental investigation into the effects of cerebral spinal fluid (CSF) in NIRS measurement of blood volume and blood oxygenation in the brain. Several papers have demonstrated that light measurement with small source-detector distances allow the majority of the signal to channel through the CSF layer in the head resulting in improper prediction of the

Table 2 Calculated values for absorption and scattering coefficients (in units of mm^{-1}) using the infinite medium spatial derivative (or multi-distance) method for different ranges of angles between the source and three detectors. For each case the spatial derivative of phase and $\ln(\rho I_{ac})$ vs distance was calculated from three detector positions, and fit to the infinite medium model. The expected values for the phantom were $\mu_a = 0.0037$ mm^{-1}, and $\mu_s' = 0.50$ mm^{-1}.

Angle range between source & detectors	μ_a (infinite medium)	μ_s' (infinite medium)
11.25–56.25°	0.0069	0.27
33.75–78.75°	0.0055	0.27
56.25–101.25°	0.0051	0.35
78.75–168.75°	0.0038	0.39
11.25–168.75°	0.0046	0.33

hemoglobin values from the measurements.[53,54] This is compounded by the fact that the diffusion model, which is often used to solve for absorption coefficients, cannot properly predict light propagation in weakly scattering media, such as the CSF. These computational and modeling studies are at odds with in vivo measurements of hematoma in the brain, which appear to yield correct values using point measurements with a source-detector spacing of less than 5 cm.[55] While this controversy is likely to continue, it is important to study further the effect of an optically clear layer of material located in the subsurface region of a tissue volume upon the measured data. Some simple phantom measurements have been carried out to assess the magnitude of effect that such a physiologic structure might have upon transmission measurements in a neonatal head phantom.

A phantom of oxygenated blood at 2 ml/L concentration by volume mixed in a solution of 0.5% Intralipid was housed in a cylindrical geometry with a radius of 45 mm. The phantom was made so that clear glass cylinders could be inserted into the medium simulating a circular layer of CSF in the head. Measurements of ac amplitude and phase were recored around the phantom to assess the effect of the clear layer. Measurements with and without the clear layers are shown in Figures 6(a) and 6(b). Two different clear cylinders were used to examine the effect of the layer, the first having an outer radius of 35 mm, with a 2 mm thickness. The second cylinder had an outer radius of 39 mm, with a 2 mm thickness. Interestingly, the measurements of ac intensity did not show much difference between measurements with or without the clear layer; however, the phase shift is markedly different when the clear cylinder was present, especially for source-detector separations directly across the cylindrical phantom. Using the slopes of phase shift and ac magnitude from these latter two data sets produces an overestimation in the absorption coefficient of 15% and 25% from the homogeneous case.

5 Discussion

Pediatric applications of NIRS appear promising because there is a niche where an accurate on-line monitor for neonatal/fetal blood volume and oxygenation would be beneficial to prevent prolonged hypoxia, acute hypoxic ischemia, or to monitor fetal cerebral hemodynamics during labor.[7-9] One of the instruments examined here has been developed to monitor the total hemoglobin blood volume and hemoglobin oxygen saturation averaged over the neonate head.[6] While some monitors measure surface reflectance or transmission through a thin tissue (such as the finger or ear), only measurement across the head, with a direct probe of the optical pathlength, can be used to quantitatively determine these values noninvasively. Calibration of this type of system requires the use of a model for calculation of the absorption coefficients from the measured values, and this study presents a potential solution to this problem. While the diffusion model has demonstrated success in this respect for reflectance based systems,[33,39,40] it has not been clear how successful it can be for transmittance based systems over long optical pathlengths.

Based upon the good agreement in the slopes of phase shift and $\ln(\rho I_{ac})$ versus distance between theory and experiment in Figures 2 and 3, it appears that this derivative method, or the "multi-distance method" as described by Franceschini
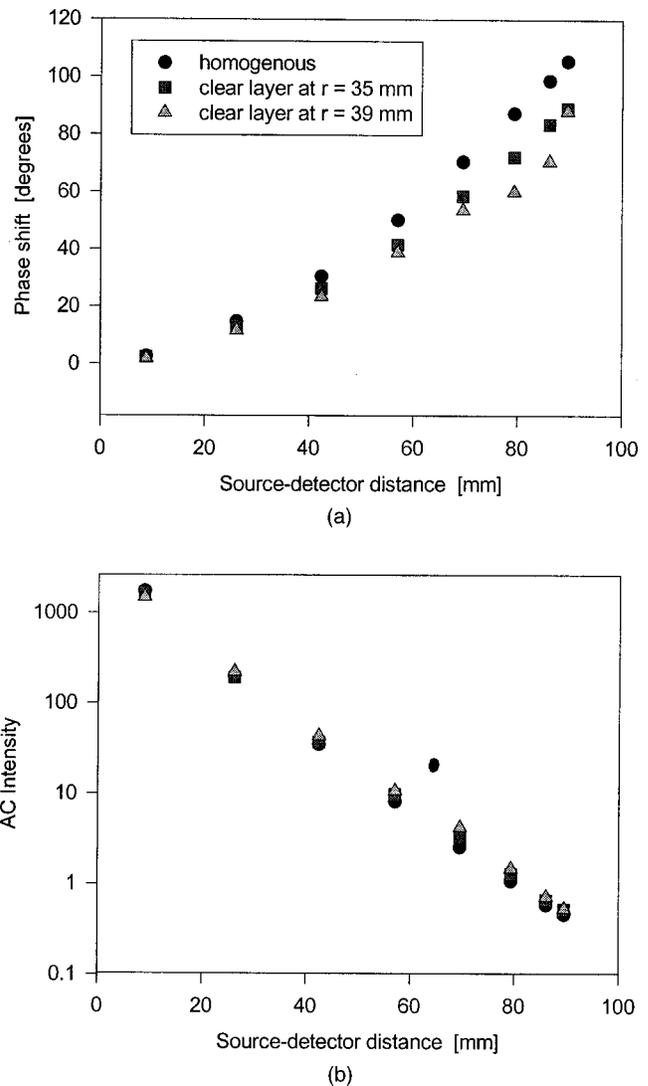
Fig. 6 Measured phase shift (a) and ac intensity (b) vs chord distance between the source and detector, for three cylindrical phantoms. The first phantom was homogenous with radius of 45.5 mm, while the second phantom was the same as the first but with an embedded clear glass cylinder having a radius of 35 mm. The third phantom was again the same as the first with a clear glass cylinder having a radius of 39 mm within the sample. Both glass cylinders were 2 mm thick and located concentrically within the phantoms.

et al.,[40] can be applied to larger cylindrical phantoms. This approach is attractive for the monitoring system described here since the infinite-medium fitting procedure can be completed in "real time" from a small data set. An interesting observation from Figure 3 is that the infinite medium derivatives fit better at longer chord distances, such that if data are used within the first 30 mm, the fitting procedure is less accurate (see Table 2 for comparison of fits at different source-detector angles). This observation is likely due to boundary effects resulting from the curved tissue surface which creates a fluence rate distribution which is much less similar to that in an infinite medium. Therefore, when using the infinite medium multi-distance method for fitting neonatal head data, the largest source-detector distance ranges should be used to avoid this geometrical problem.

The differential pathlength factor method described by Cope and Delpy works well estimating absolute changes in the absorption coefficient, however it appears to be limited by a constant offset in the measurement which is related to measurement geometry. Further study of this constant offset factor may lead to a scheme for minimizing its effect. Application of this method for absorption coefficient changes appears to be quite robust, and easy to use.

The finite element fitting procedure routinely provides accurate estimates of the phantom optical properties, and previous studies have proven this over a large range of physiologically relevant optical properties.[45] While this fitting procedure is robust, it requires more time than the analytic methods, and will likely not be used for on-line monitoring. It is quite possible that the range of physiologic optical property data sets to be encountered could be pre-calculated with the finite element method and the values retained in a look-up data table. This would provide a fast on-line system for estimating tissue optical properties which could be potentially more accurate than the infinite medium method; however, it is not clear how either of these techniques would respond to noncylindrical tissue shapes or other boundary effects such as dark hair. These potentially confounding issues remain for future study. Our preliminary investigation of the effect of a nonscattering layer embedded in a phantom provides some insight into the problem that such a layer produces. Interestingly, the layer does not appear to significantly impact the measurement of ac magnitude, but it does decrease the observed phase shift. Also, these effects are most significant at the furthest source-detector distances, in contrast to the predictions by Firbank, Schweiger, and Delpy.[53,54] This discrepancy may be due to the differing indicies of refraction of glass and water; however, one would not expect such a phase shift difference based upon this. Perhaps the most important observation from this data is that the nonscattering layer produces an overestimation of the absorption coefficient by lowering the phase shift. The magnitude of this effect *in vivo* remains to be quantified, and further study of the problem is critical to the development of absolute quantitative optical monitoring for clinical use.

6 Conclusions

In summary, we have demonstrated that: (1) the modified Beer–Lambert law method described by Cope and Delpy[13,36] can be used to quantify absolute changes in the absorption coefficient across a large tissue-simulating cylinder, (2) the infinite medium multi-distance method described by Fantini and Franceschini[33,39,40] can be used to accurately estimate the absolute absorption coefficient across a large tissue-simulating cylinder, and (3) the finite element method by Paulsen and Jiang[43] can also be used to quantitatively estimate the absolute absorption coefficient of large tissue-simulating cylinders. When the infinite-medium multi-distance method is used, the optical properties are recovered more accurately from measurements at large source-detector distances which minimize the effect of the curved tissue surface. This approach can provide a fast and computationally efficient method for on-line monitoring of the absorption due to hemoglobin at multiple wavelengths across the neonate head.

References

1. W. A. Bowes, B. C. Corke, and J. Hulka, ''Pulse oximetry: a review of the theory, accuracy, and clinical applications,'' *Obstet. Gynecol. (N.Y.)* **74**(3), 541–546 (1989).
2. K. Dziedzic and D. Vidyasagar, ''Pulse oximetry in neonatal intensive care,'' *Clin. Perinatol* **16**(1), 177–197 (1989).
3. B. Chance, S. Nioka, J. Kent, K. McCully, M. Foutain, R. Greenfield, and G. Holtom, ''Time-resolved spectroscopy of hemoglobin and myoglobin in resting and ischemic muscle,'' *Anal. Biochem.* **174**, 698–707 (1988).
4. R. A. De Blasi, S. Fantini, M. A. Franceschini, M. Ferrari, and E. Gratton, ''Cerebral and muscle oxygen saturation measurement by frequency-domain near-infrared spectrometer,'' *Med. Biol. Eng. Comput.* **33**(2), 228–230 (1995).
5. M. Cope and D. T. Delpy, ''System for long-term measurement of cerebral blood and tissue oxygenation on newborn infants by near-infrared transillumination,'' *Med. Biol. Eng. Comput.* Vol. **26**, 289–294 (1988).
6. J. E. Brazy, ''Cerebral oxygen monitoring with near infrared spectroscopy: Clinical application to neonates,'' *J. Clin. Monitor* **7**(4), 325–334 (1991).
7. P. Rolfe, Y. A. Wickramasinghe, M. S. Thornley, F. Faris, R. Houston, R. Kai, K. Yamakoshi, S. O'Brien, M. Doyle, and K. Palmer, ''Fetal and neonatal cerebral oxygen monitoring with NIRS: Theory and practice,'' *Early Hum. Dev.* **29**(1–3), 269–273 (1992).
8. P. M. Doyle, S. O'Brien, Y. A. Wickramasinghe, R. Houston, and P. Rolfe, ''Near infrared spectroscopy used to observe changes in fetal cerebral haemodynamics during labour,'' *J. Perinat. Med.* **22**(3), 265–268 (1994).
9. J. A. Low, ''Cerebral perfusion, metabolism, and outcome,'' *Curr. Opin. Pediatr.* **7**(2), 132–139 (1995).
10. U. Elchalal, A. Weissman, A. Abramov, D. Abramov, and D. Weissman, ''Intrapartum fetal pulse oximetry—present and future,'' *Int. J. Gyn. Obst.* **50**(2), 131–137 (1995).
11. K. J. Sapire, S. P. Gopinath, G. Farhat, D. R. Thakar, A. Gabrielli, J. W. Jones, R. S. Robertson, and B. Chance, ''Cerebral oxygenation during warming after cardiopulmonary bypass,'' *Crit. Care Med.* **25**, 1655–1662 (1997).
12. T. J. Germon, A. E. R. Young, A. R. Manara, and R. J. Nelson, ''Extracerebral absorption of near-infrared light influences on the detection of increased cerebral oxygenation monitored by near-infrared spectroscopy,'' *J. Neurol., Neurosurg. Psychiatry* **58**(4), 477–479 (1995).
13. D. T. Delpy and M. Cope, ''Quantification in tissue near-infrared spectroscopy,'' *Philos. Trans. R. Soc. London, Ser. B* **352**, 649–659 (1997).
14. L. Y. Gibson, ''Pulse oximeter in the neonatal ICU: A correlational analysis,'' *Pediatr. Nurs.* **22**(6), 511–515 (1996).
15. E. H. Thilo, D. Andersen, M. L. Wasserstein, J. Schmidt, and D. Luckey, ''Saturation by pulse oximetry: Comparison of the results obtained by instruments of different brands,'' *J. Pediatr. (St. Louis)* **122**(4), 620–626 (1993).
16. C. E. Elwell, H. Owen-Reece, M. Cope, and D. T. Delpy, ''Measurement of adult cerebral haemodynamics using near infrared spectroscopy,'' *Acta Neurochir. Suppl.* **59**, 74–80 (1993).
17. V. Pollard, D. S. Prough, A. E. DeMelo, D. J. Deyo, T. Uchida, and H. F. Stoddart, ''Validation in volunteers of a near-infrared spectroscope for monitoring brain oxygenation in vivo,'' *Anesth. Analg (Baltimore)* **82**(2), 269–277 (1996).
18. W. N. J. N. Colier, N. J. C. W. van Haaren, and B. Oeseburg, ''A comparative study of 2 near-infrared spectrophotometers for the assessment of cerebral hemodynamics,'' *Acta Anaesthesiol.* **39**, 101–105 (1995).
19. E. G. McKeating, J. R. Monjardino, D. F. Signorini, M. J. Souter, and

P. Andrews, ''A comparison of the Invos 3100 and the Critikon 2020 near-infrared spectrophotometers as monitors of cerebral oxygenation,'' *Anaesthesia* **52**(2), 136–140 (1997).

20. G. Buunk, J. G. van der Hoeven, and A. E. Meinders, ''A comparison of near-infrared spectroscopy and jugular bulb oximetry in comatose patients resuscitated from a cardiac arrest,'' *Anaesthesia* **53**(1), 13–19 (1998).

21. J. A. Wahr, K. K. Tremper, S. Samra, and D. T. Delpy, ''Near-infrared spectroscopy: Theory and applications,'' *J. Cardiothorac Vasc. Anesth.* **10**(3), 406–418 (1996).

22. A. Duncan, J. H. Meek, M. Clemence, C. E. Elwell, P. Fallon, L. Tyszczuk, M. Cope, and D. T. Delpy, ''Measurement of cranial optical path length as a function of age using phase resolved near infrared spectroscopy,'' *Pediatr. Res.* **39**(5), 889–894 (1994).

23. C. D. Kurth and B. Uher, ''Cerebral hemoglobin and optical pathlength influence on near-infrared spectroscopy measurement of cerebral oxygen saturation,'' *Anesth. Analg. (Baltimore)* **84**(6), 1297–1305 (1997).

24. M. Essenpreis, M. Cope, C. E. Elwell, S. R. Arridge, P. van der Zee, and D. T. Delpy, ''Wavelength dependence of the differential pathlength factor and the log slope in time-resolved tissue spectroscopy,'' *Adv. Exp. Med. Biol.* **333**, 9–20 (1993).

25. S. J. Matcher, C. E. Elwell, C. E. Cooper, M. Cope, and D. T. Delpy, ''Performance comparison of several published tissue near-infrared spectroscopy algorithms,'' *Anal. Biochem.* **227**(1), 54–68 (1995).

26. C. E. Cooper, C. E. Elwell, J. H. Meek, J. H. Matcher, S. J. Wyatt, J. S. M. Cope, and D. T. Delpy, ''The noninvasive measurement of absolute cerebral deoxyhaemoglobin concentration and mean optical pathlength in the neonatal brain by second derivative near infrared spectroscopy,'' *Pediatr. Res.* **39**, 32–38 (1996).

27. C. D. Kurth, H. Liu, W. S. Thayer, and B. Chance, ''A dynamic phantom brain model for near-infrared spectroscopy,'' *Phys. Med. Biol.* **40**(12), 2079–92 (1995).

28. S. J. Matcher and C. E. Cooper, ''Absolute quantification of deoxy-haemoglobin concentration in tissue using near infrared spectroscopy,'' *Phys. Med. Biol.* **39**, 1295 (1994).

29. B. Chance, J. S. Leigh, H. Miyake, D. Smith, S. Nioka, R. Greenfield, M. Finander, K. Kaufman, W. Levy, M. Young, P. Cohen, H. Yoshioka, and R. Boretsky, ''Comparison of time-resolved and unresolved measurements of deoxyhemoglobin in brain,'' *Proc. Natl. Acad. Sci. USA* **85**, 4971 (1988).

30. D. T. Delpy, M. Cope, P. van der Zee, S. R. Arridge, S. Wray, and J. S. Wyatt, ''Estimation of optical pathlength through tissue from direct time of flight measurement,'' *Phys. Med. Biol.* **33**, 1433–1442 (1988).

31. M. S. Patterson, B. Chance, and B. C. Wilson, ''Time resolved reflectance and transmittances for the noninvasive measurement of tissue optical properties,'' *Appl. Opt.* **28**, 2331–2336 (1989).

32. M. S. Patterson, J. D. Moulton, B. C. Wilson, K. W. Berndt, and J. R. Lakowicz, ''Frequency-domain reflectance for the determination of the scattering and absorption properties of tissue,'' *Appl. Opt.* **30**(24), 4474–4476 (1991).

33. S. Fantini, M. A. Franceschini, J. Fishkin, B. Barbieri, and E. Gratton, ''Quantitative determination of the absorption spectra of chromophores in strongly scattering media: A light emitting diode based technique,'' *Appl. Opt.* **33**, 5204–5213 (1993).

34. S. J. Madsen, E. R. Anderson, R. C. Haskell, and B. J. Tromberg, ''Portable, high-bandwidth frequency-domain photon migration instrument for tissue spectroscopy,'' *Opt. Lett.* **19**(23), 1934–1936 (1994).

35. B. W. Pogue and M. S. Patterson, ''Frequency domain optical absorption spectroscopy of finite tissue volumes using diffusion theory,'' *Phys. Med. Biol.* **39**, 1157 (1992).

36. M. Cope, ''The application of near infrared spectroscopy to non invasive monitoring of cerebral oxygenation in the newborn infant,'' PhD thesis, University College of London, 1991.

37. M. Cope, P. van der Zee, M. Essenpreis, S. R. Arridge, and D. T. Delpy, ''Data analysis methods for near infrared spectroscopy of tis-sues: problems in determining the relative cytochrome of tissues,'' *Proc. SPIE* **1431**, 251–263 (1991).

38. S. R. Arridge, M. Cope, and D. T. Delpy, ''The theoretical basis for the determination of optical pathlengths in tissue: Temporal and frequency analysis,'' *Phys. Med. Biol.* **37**(7), 1531–1560 (1992).

39. S. Fantini, M. A. Franceschini-Fantini, S. A. Walker, B. Barbieri, and E. Gratton, ''Frequency-domain multichannel optical-detector for noninvasive tissue spectroscopy and oximetry,'' *Opt. Eng.* **34**(1), 32–42 (1995).

40. M. A. Franceschini, S. Fantini, L. A. Paunescu, J. Maier, and E. Gratton, ''Influence of a superficial layer in the quantitative spectroscopic study of strongly scattering media,'' *Appl. Opt.* **37**(31), 7447–58 (1998).

41. S. R. Arridge, P. van der Zee, M. Cope, and D. T. Delpy, ''Reconstruction methods for infrared absorption imaging,'' *Proc. SPIE* **1431**, 204–215 (1991).

42. B. W. Pogue, M. S. Patterson, H. Jiang, and K. Paulsen, ''Initial assessment of a simple system for frequency domain diffuse optical tomography,'' *Phys. Med. Biol.* **40**, 1709–1729 (1995).

43. K. D. Paulsen and H. Jiang, ''Spatially varying optical property reconstruction using a finite element diffusion equation approximation,'' *Med. Phys.* **22**(6), 691–701 (1995).

44. B. W. Pogue, M. Testorf, T. McBride, U. Osterberg, and K. Paulsen, ''Instrumentation and design of a frequency-domain diffuse optical tomography imager for breast cancer detection,'' *Opt. Express* **1**(13), 391–403 (1997).

45. T. O. McBride, B. W. Pogue, E. Gerety, S. Poplack, U. L. Osterberg, and K. D. Paulsen, ''Spectroscopic diffuse optical tomography for the quantitative assessment of hemoglobin concentration and oxygenation in breast tissue,'' *Appl. Opt.* **38**(25), 5480–90 (1999).

46. H. J. van Staveren, C. J. M. Moes, J. van Marle, S. A. Prahl, and M. J. C. van Gemert, ''Light scattering in Intralipid-10% in the wavelength range of 400–1100 nm,'' *Appl. Opt.* **30**(31), 4507–4514 (1991).

47. S. Wray, M. Cope, D. T. Delpy, J. Wyatt, and E. Reynolds, ''Characterization of the near infrared absorption spectra of cytochrome $aa3$ and haemoglobin for the non-invasive monitoring of cerebral oxygenation,'' *Biochem. Biophys. Acta* **933**, 184–192 (1988).

48. M. Cope and D. T. Delpy, ''System for long-term measurement of cerebral blood and tissue oxygenation on newborn infants by near-infrared transillumination,'' *Med. Biol. Eng. Comput.* **26**, 289–294 (1988).

49. D. T. Delpy, M. Cope, P. van der Zee, S. Arridge, S. Wray, and J. S. Wyatt, ''Estimation of optical pathlength through tissue from direct time of flight measurement,'' *Phys. Med. Biol.* **33**, 1433–1442 (1988).

50. J. D. Moulton, ME thesis, ''Diffusion theory modelling of picosecond laser pulse generation propagation in turbid media,'' McMaster University, 1990.

51. M. S. Patterson, ''Principles and applications of frequency-domain measurements of light propagation,'' in *Optical-Thermal Response of Laser-Irradiated Tissue*, A. J. Welch and M. J. C. van Gemert, Eds., pp. 333–364, Plenum, New York (1995).

52. W. F. Cheong, S. A. Prahl, and A. J. Welch, ''A review of the optical properties of biological tissues,'' *IEEE J. Quantum Electron.* **26**(12), 2166–2185 (1990).

53. M. Firbank, M. Schweiger, and D. T. Delpy, ''Investigation of 'light piping' through clear regions of scattering objects,'' *Proc. SPIE* **2389**, 167–173 (1995).

54. M. Firbank, S. R. Arridge, M. Schweiger, and D. T. Delpy, ''An investigation of light transport through scattering bodies with non-scattering regions,'' *Phys. Med. Biol.* **41**, 767–783 (1996).

55. B. Chance, Q. Luo, S. Nioka, D. C. Alsop, and J. A. Detre, ''Optical investigations of physiology: A study of intrinsic and extrinsic biomedical contrast,'' *Philos. Trans. R. Soc. London, Ser. B* **352**, 707–716 (1997).